

Evidence for suppression of structure growth in the concordance cosmological model

Nhat-Minh Nguyen^{DOI},^{*} Dragan Huterer^{DOI},[†] and Yuewei Wen^{DOI}

*Leinweber Center for Theoretical Physics, University of Michigan, 450 Church St, Ann Arbor, MI 48109-1040 and
Department of Physics, College of Literature, Science and the Arts,
University of Michigan, 450 Church St, Ann Arbor, MI 48109-1040*

(Dated: February 3, 2023)

We present evidence for a suppressed growth rate of large-scale structure during the dark-energy dominated era. Modeling the growth rate of perturbations with the “growth index” γ , we find that current cosmological data strongly prefer a higher growth index than the value $\gamma = 0.55$ predicted by general relativity in a flat Λ CDM cosmology. Both the cosmic microwave background data from Planck and the large-scale structure data from weak lensing, galaxy clustering, and cosmic velocities separately favor growth suppression. When combined, they yield $\gamma = 0.633^{+0.025}_{-0.024}$, excluding $\gamma = 0.55$ at a statistical significance of 3.7σ . The combination of $f\sigma_8$ and Planck measurements prefers an even higher growth index of $\gamma = 0.639^{+0.024}_{-0.025}$, corresponding to a 4.2σ -tension with the concordance model. In Planck data, the suppressed growth rate offsets the preference for nonzero curvature and fits the data equally well as the latter model. A higher γ leads to a higher matter fluctuation amplitude S_8 inferred from galaxy clustering and weak lensing measurements, and a lower S_8 from Planck data, effectively resolving the S_8 tension.

Introduction. The flat Λ CDM concordance cosmology, which combines general relativity (GR) and a spatially flat universe with $\sim 70\%$ constant dark energy and $\sim 30\%$ cold dark matter, provides an excellent fit to observational data. However, several tensions in measurements of parameters in this model have been noted in recent years [1]. Most significantly, the expansion rate H_0 inferred from the distance ladder [2] is higher than that measured by the cosmic microwave background (CMB) [3]. At a lesser level of significance, the parameter $S_8 \equiv \sigma_8 \sqrt{\Omega_m}/0.3$ (where σ_8 is the amplitude of mass fluctuations in spheres of $8 h^{-1}\text{Mpc}$ and Ω_m is matter density relative to the critical density) determined by CMB observations is larger than that found by galaxy clustering and weak gravitational lensing measurements [4]. Finally, the Planck CMB data by itself shows a preference for a nonzero spatial curvature Ω_K [3].

In this Letter, we consider the possibility that the growth of structure deviates from what predicted by the concordance model. While it is true that all the aforementioned parameters (Ω_m , S_8 , and Ω_K) affect the growth of density perturbations, they also control geometrical quantities like distances and volumes, complicating the physical interpretation. It is thus important to isolate and constrain the growth of structure [5] separately from geometrical quantities. Here, we adopt a precise parameterization of the growth rate and find evidence for growth suppression — relative to the expectation from flat Λ CDM and GR — which also reconciles tensions in S_8 and Ω_K constraints. Our results clarify and consolidate the current situation in the field, where different analyses adopting different prescriptions of growth, or different implementations of how growth is separated from geometry, either found some evidence for a suppressed growth [6–15] or did not [16–22].

Growth of structure. Over cosmic time, matter

density fluctuations $\delta \equiv (\rho - \bar{\rho})/\bar{\rho}$ (where ρ and $\bar{\rho}$ are the local and the cosmic mean densities respectively) are amplified by gravity. Assuming GR and restricting to linear regime where $\delta \ll 1$ (roughly $k \lesssim 0.1 h \text{ Mpc}^{-1}$ today with $h = H_0/100 \text{ km s}^{-1} \text{ Mpc}^{-1}$) and subhorizon scales (roughly $k \gtrsim H_0 \simeq 0.0003 h \text{ Mpc}^{-1}$ today), we can describe the growth of large-scale structure as [23, 24]

$$\ddot{\delta}(\mathbf{k}, t) + 2H\dot{\delta}(\mathbf{k}, t) - 4\pi G\bar{\rho}\delta(\mathbf{k}, t) = 0, \quad (1)$$

where dot denotes derivative with respect to time. Here the matter overdensity δ , the expansion rate H , and the mean matter density $\bar{\rho}$ all depend on time, while every Fourier \mathbf{k} -mode evolves independently. In this regime, it is useful to consider the (linear) growth function $D(t) \equiv \delta(t)/\delta(t_0)$, where t_0 is the present time, and the growth rate $f(a) \equiv d \ln D(a)/d \ln a$, where $a(t)$ is the scale factor. The growth rate is a central link between data and theory: it is directly proportional to large-scale structure observables like peculiar velocities and redshift-space distortions [25, 26], while being exquisitely sensitive to the properties of dark-energy models [27].

To further isolate the temporal evolution of structure, [28–30] introduced a robust and accurate approximation of the growth rate as

$$f(a) = \Omega_m^\gamma(a), \quad (2)$$

where γ is the *growth index*. In particular, [29, 30] showed that standard GR in the flat Λ CDM background predicts $\gamma \simeq 0.55$ even in the presence of dark energy; this fit is accurate to $\simeq 0.1\%$ [30–32]. A measured deviation from $\gamma = 0.55$ would suggest an inconsistency between the concordance cosmological model and observations. Assuming Eq. (2), the linear growth function takes the form

$$D(\gamma, a) = \exp \left[- \int_a^1 da \frac{\Omega_m^\gamma(a)}{a} \right], \quad (3)$$

where we have normalized $D(\gamma, a = 1) \equiv 1$ for all γ . A $\gamma > 0.55$ corresponds to a growth rate $f(\gamma, a) < f(0.55, a)$ and, because of the normalization, to a growth function $D(\gamma, a) > D(0.55, a)$ in the past.

Methodology and data. To implement Eqs. (2)–(3), we express the linear matter power spectrum as

$$P(\gamma, k, a) = P_{\text{today}}(k, a = 1) D^2(\gamma, a), \quad (4)$$

where P_{today} is the fiducial linear matter power spectrum evaluated today which depends on the usual set of cosmological parameters. To compute transfer functions and power spectra, we modify the cosmological Boltzmann solver CAMB [33, 34]. With $\gamma = 0.55$ we obtain (at redshift $z = 1.5$ and up to $k \lesssim 0.1 h \text{ Mpc}^{-1}$) linear matter power spectra within 0.1% of the outputs from the unmodified version of CAMB. Likewise, we repeat the baseline Planck 2018 [3] and DES year-1 [35] analyses, using our modified CAMB [36] at fixed $\gamma = 0.55$, and reproduce their constraints on relevant cosmological parameters well within their precision.

Because the growth-index parameterization has only been validated for sub-horizon perturbations, care needs to be taken when modeling the CMB whose information partially comes from large scales and high redshifts. We choose to exempt the primary CMB anisotropies from the growth-index description. That is, we ensure Eq. (4) does not directly alter the *unlensed* CMB power spectra, but rather only affects the lensing effect, i.e. smoothing of the primary CMB acoustic peaks. Consequently, CMB data is sensitive to γ only through the CMB lensing gravitational potential [37], which is generated by density fluctuations within the regime where Eqs. (2)–(4) are valid.

Our baseline data includes measurements of the parameter combination $f\sigma_8$ from peculiar velocity and redshift-space distortion (RSD) data, at local ($z < 0.1$) [10, 38–41] and cosmological distances ($z \geq 0.1$) [42–47]. Fig. 2 shows these $f\sigma_8$ measurements at the corresponding redshifts. We assume that the $f\sigma_8$ measurement uncertainties are Gaussian-distributed and uncorrelated among each other [48]. We further complement the $f\sigma_8$ measurements with either the Planck 2018 CMB data — including temperature, polarization and lensing reconstruction [3, 49] (hereafter PL18) — or large-scale structure data from galaxy surveys, or both. Data from galaxy surveys include a) the DESY1 3x2pt correlation functions [35] (hereafter DESY1), and b) baryon acoustic oscillations in the 6dF Galaxy Survey (6dFGS) galaxy [50] and the Sloan Digital Sky Survey (SDSS) [47, 51, 52] galaxy plus Lyman-alpha (hereafter BAO collectively). When including both SDSS $f\sigma_8$ and BAO data, we employ joint covariance and likelihood that properly account for their correlations [53]. Throughout, we adopt the same likelihoods and priors used in the baseline of those analyses. We fix the total mass of neutrinos to $\sum m_\nu = 0.06$ eV and include neutrino contribution Ω_ν in the matter

density parameter Ω_m . We verify that excluding Ω_ν in computing theoretical $f\sigma_8$ leads to negligible changes in the latter and all downstream results. We allow γ to vary assuming a uniform prior $\mathcal{U}(0, 2.0)$.

We wish to constrain the growth index γ , along with other standard cosmological parameters: the matter and baryon densities relative to critical Ω_m and Ω_b , the Hubble constant H_0 , spectral index n_s , mass fluctuation amplitude σ_8 , and reionization optical depth τ . We therefore perform Bayesian inference via the Monte Carlo Markov Chain (MCMC) method using the `cobaya` framework [54] and analyze the MCMC samples using the `GetDist` package [55].

To quantify the statistical significance of our results, we compute the Bayesian factor of $\gamma = 0.55$ and $\gamma \neq 0.55$ by assuming the Savage-Dickey density ratio

$$\log_{10} \text{BF}_{01} = \log_{10} \left. \frac{\mathcal{P}(\gamma|d, M_1)}{\mathcal{P}(\gamma|M_1)} \right|_{\gamma=0.55}, \quad (5)$$

where d and M_1 respectively denote the data and the model with γ , while $\mathcal{P}(\gamma|M_1) = \mathcal{U}(0., 2.)$. This is reported in the fifth column of Tab. I. We further quote the significance of $\gamma \neq 0.55$ following the two-tailed test and measuring the posterior tail in units of Gaussian sigmas. To compare the goodness of fit between models, we first identify best-fit models that maximize their corresponding joint posteriors, then report the chi-square difference $\Delta\chi^2$ between two such models in the last column of Tab. I and in Tab. II.

Constraints on γ in a flat universe. We first consider the data combination $f\sigma_8 + \text{PL18}$. Marginalizing over all other cosmological parameters, we obtain the posterior density of γ shown in orange in Fig. 1. This corresponds to the constraint $\gamma = 0.639^{+0.024}_{-0.025}$ and a Bayes factor of $|\log_{10} \text{BF}_{01}| = 1.7$. The former excludes $\gamma = 0.55$ at a statistical significance of 4.2σ , while the latter provides a “very strong” evidence for deviation from the GR+flat ΛCDM prediction of $\gamma = 0.55$ according to the Jeffreys’ scale [56]. Note that neither PL18 nor $f\sigma_8$ alone substantially constrains the growth index due to degeneracies with other cosmological parameters, yet together they show a clear preference for $\gamma > 0.55$, that is, a lower rate of growth than predicted by GR in flat ΛCDM . Fig. 2 illustrates the effect of growth suppression as a function of redshift by showing the $f\sigma_8(z)$ posterior assuming flat ΛCDM , and that assuming flat $\Lambda\text{CDM} + \gamma$, both inferred from the $f\sigma_8 + \text{PL18}$ data combination.

We next wish to investigate how the large-scale structure clustering and lensing data constrain γ . To do so, we replace the PL18 data by the DESY1 3x2pt measurements of galaxy clustering and weak lensing, together with the expansion-history data from BAO. The $f\sigma_8 + \text{DESY1} + \text{BAO}$ data combination yields the marginalized constraint $\gamma = 0.598^{+0.031}_{-0.031}$. Much like the $f\sigma_8 + \text{PL18}$ constraint, this combination prefers a higher

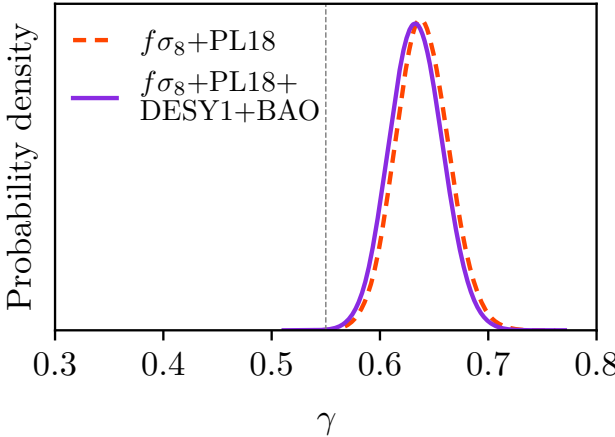


FIG. 1. Marginalized constraints on the growth index γ , from $f\sigma_8$ data combined with PL18 (orange) and PL18+DESY1+BAO (violet). The vertical dashed line marks the concordance model prediction of $\gamma = 0.55$.

growth index than the GR value, except now at a lower statistical significance, excluding $\gamma = 0.55$ at 2.0σ .

We finally report the constraint from all data combined, $f\sigma_8 + \text{PL18} + \text{DESY1} + \text{BAO}$:

$$\gamma = 0.633^{+0.025}_{-0.024}. \quad (6)$$

Analysis of the posterior tails indicates that $\gamma = 0.55$ is excluded at 3.7σ , while the Bayes factor $|\log_{10} \text{BF}| = 1.2$ shows a “strong” evidence for a departure from the expected value of γ . We show the posterior density of γ for combined data in violet in Fig. 1; it is very close to the posterior for $f\sigma_8 + \text{PL18}$.

We summarize all marginalized constraints on γ , together with their statistical significance, in Tab. I.

Implications for S_8 tension. A moderate yet persistent tension in constraints of S_8 has emerged between CMB measurements, e.g. Planck [3] or Atacama Cosmology Telescope plus Wilkinson Microwave Anisotropy Probe [57], and low-redshift 3x2pt measurements of weak lensing and galaxy clustering, e.g. the Dark Energy Survey (DES) [35], the Kilo-Degree Survey (KiDS) [58], and combinations thereof [59]. This discrepancy is statistically significant and unlikely to be explained by lensing systematics alone [60], thus motivates investigations of physics beyond the standard model.

Fig. 3 shows the marginalized constraints in the 2D planes of the growth index γ and, from left to right, S_8 or Ω_m or H_0 , by different data combinations. Notably, the $S_8 - \gamma$ panel indicates a potential solution to the S_8 tension: a higher growth index ($\gamma \simeq 0.65$) implies a *higher* S_8 value in the probes of large-scale structure. Specifically, the $f\sigma_8 + \text{DESY1} + \text{BAO}$ combination yields $S_8 = 0.784^{+0.017}_{-0.016}$, while in the standard ΛCDM (with $\gamma \equiv 0.55$) $S_8 = 0.771^{+0.014}_{-0.014}$. Conversely, Planck now prefers a *lower*

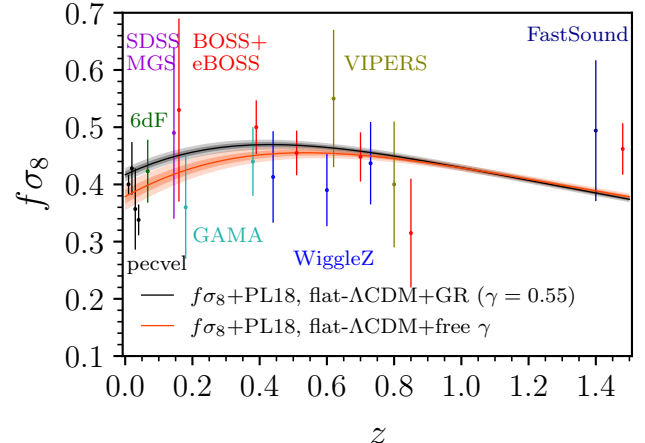


FIG. 2. Marginalized posterior on the theoretical $f\sigma_8(z)$ assuming the growth-index parameterization in Eq. (2). Shaded bands show the 68% and 95% posteriors from our baseline analysis that includes $f\sigma_8$ and PL18 data (orange), and the corresponding constraints in the concordance model with $\gamma = 0.55$ (black). The data points indicate actual $f\sigma_8$ measurements.

amplitude of fluctuations ($S_8 = 0.807^{+0.019}_{-0.019}$) than it does in ΛCDM ($S_8 = 0.831^{+0.013}_{-0.012}$). Consequently, the “ S_8 tension” between the measurements of S_8 in the galaxy clustering and gravitational lensing versus that in Planck decreases from 3.2σ to 0.9σ , as measured by the S_8 difference divided by errors added in quadrature.

Allowing curvature to vary. Relaxing the assumption of spatial flatness changes the expansion history and the concordance prediction for the growth history [61, 62]. An immediate question is whether the apparent preference for a higher growth index and a slower growth rate is the same effect as the apparent preference for a nonzero curvature found by the Planck 2018 analysis that, by using temperature and polarization data, found $\Omega_K = -0.044^{+0.018}_{-0.015}$ ([3]; see also [63, 64]).

Allowing both curvature and growth index to vary, we observe a trade-off between Ω_K and γ , as shown in Fig. 4 using *only* Planck CMB temperature and polarization data (henceforth PL18 temp.+pol.). The data clearly prefer either a positively curved space, i.e. $\Omega_K < 0$, or growth suppressed relative to the GR prediction, i.e. $\gamma > 0.55$; the flat model with $\gamma = 0.55$ has a worse fit than the best-fit model by $\Delta\chi^2 = -6.9$.

We next focus on two limits of the results shown in Fig. 4: a) varying Ω_K while fixing $\gamma = 0.55$ (which reproduces the standard analysis from the Planck paper, also finding $\Omega_K = -0.044$), and b) fixing $\Omega_K = 0$ while varying γ . We are particularly interested in comparing the fit of these two models. We find that the model with free curvature fits the PL18 temp.+pol. data marginally better than the model with free γ ($\Delta\chi^2 = -1.3$). Includ-

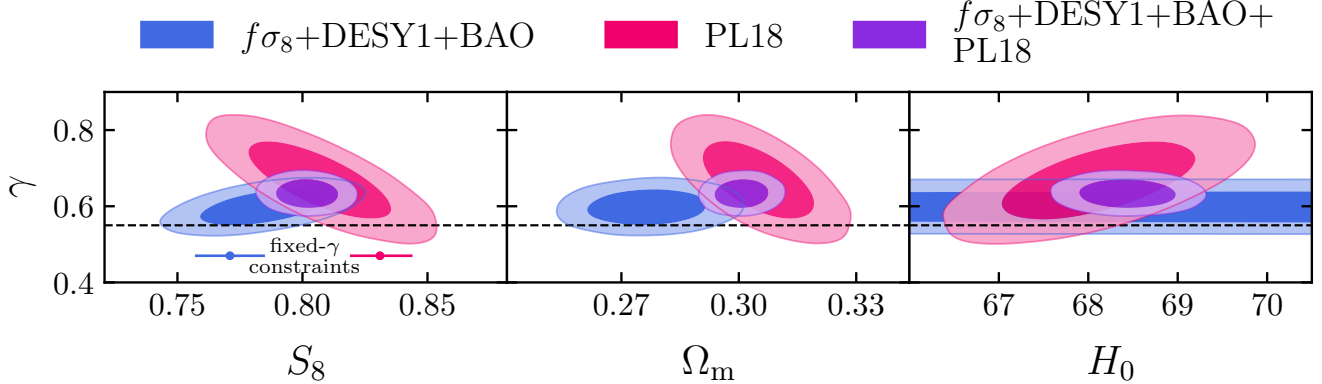


FIG. 3. 68% and 95% marginalized constraints on parameters in the concordance model allowing for a free growth index γ , from $f\sigma_8$ +DESY1+BAO (blue), PL18 alone (red) and $f\sigma_8$ +DESY1+BAO+PL18 (violet). Contours contain 68% and 95% of the corresponding projected 2D constraints. The horizontal black dashed lines mark the concordance model prediction of $\gamma = 0.55$. The horizontal bars in the $\gamma - S_8$ panel indicate the 68% limits on S_8 for a fixed $\gamma = 0.55$ (see text); they are vertically offset from $\gamma = 0.55$ for visibility.

TABLE I. Constraints on the growth index γ and cosmological parameters S_8 and H_0 from different data combinations, the corresponding Bayes factors, and chi-square differences relative to the concordance model ($\gamma = 0.55$).

Data	γ	S_8	H_0 [km s $^{-1}$ Mpc $^{-1}$]	$ \log_{10} \text{BF}_{10} $	$\Delta\chi^2 \equiv \chi^2_\gamma - \chi^2_{\gamma=0.55}$
PL18	0.668$^{+0.068}_{-0.067}$	$0.807^{+0.019}_{-0.019}$	$68.1^{+0.7}_{-0.7}$	0.4	-2.8
PL18+ $f\sigma_8$	0.639$^{+0.024}_{-0.025}$	$0.814^{+0.011}_{-0.011}$	$67.9^{+0.5}_{-0.5}$	1.7	-13.6
PL18+ $f\sigma_8$ +DESY1+BAO	0.633$^{+0.025}_{-0.024}$	$0.802^{+0.008}_{-0.008}$	$68.4^{+0.4}_{-0.4}$	1.2	-13.2
PL18+ $f\sigma_8$ +DESY1+BAO (flat Λ CDM+GR)	0.55	$0.803^{+0.008}_{-0.008}$	$68.5^{+0.4}_{-0.4}$	-	0

ing PL18 CMB lensing reconstruction likelihood leads to $\Delta\chi^2 = 0.7$ in favor of the free- γ model. Overall, we conclude that both models fit the PL18 data equally well.

Recall that the feature in the PL18 temp.+pol. data driving the preference for $\Omega_K < 0$ is essentially the same one that favors a high CMB lensing amplitude, i.e. $A_{\text{lens}} > 1$ [3, 49, 65]. Does the cosmological model with a high γ produce similar features in the CMB power spectra as those with $\Omega_K < 0$ or $A_{\text{lens}} > 1$? The answer is affirmative, as shown in Fig. 5 where we compare the residuals in the CMB temperature angular power spectrum (TT) of a) the PL18 data, b) the best-fit flat model with γ , c) the best-fit model with curvature but fixed $\gamma = 0.55$, and d) the best-fit flat model with A_{lens} but fixed $\gamma = 0.55$, all relative to that of the best-fit concordance model. All three best-fit model residuals display the same oscillatory pattern that closely follows the oscillations in the data residuals. The similarity of the effects of $\gamma > 0.55$ and $A_{\text{lens}} > 1$ in the CMB temperature and polarization power spectrum is not entirely surprising: a higher γ encodes a lower growth rate $f(a)$ and, for a fixed amount of structure observed today, a larger amount in the recent past (see Eq. (3) and the discussion that fol-

lows). This in turn implies a higher lensing signal in the CMB, and thus has a qualitatively similar effect as $A_{\text{lens}} > 1$ [66].

Summary and Discussion. In this Letter, we have presented new constraints on the growth rate using a combination of Planck, DES, BAO, redshift-space distortion and peculiar velocity measurements. The constraints from different data combinations are consistent with one another within 1σ . Our constraints exclude the predictions of flat Λ CDM model in GR at the statistical significance of 3.7σ , indicating a suppression of growth rate during the dark-energy dominated epoch.

Further, we have explicitly demonstrated that cosmological models with a high γ resolve two known tensions in cosmology. First, allowing for a suppressed growth removes the need for negative curvature indicated by the PL18 temp.+pol. data; in fact, the best-fit flat model with free γ fits the data equally well as the best-fit model with standard growth and negative curvature, producing highly similar features in the temperature angular power spectrum. Second, the discrepancy in the measured amplitude of mass fluctuations parameter S_8 from the PL18

TABLE II. Chi-square differences between best-fit models with free γ and best-fit concordance models, for different data combinations and individual likelihoods.

Data	$\Delta\chi^2 \equiv \chi^2_\gamma - \chi^2_{\gamma=0.55}$							
	low- ℓ TT	low- ℓ EE	high- ℓ TTTEE	lensing	$f\sigma_8$	DESY1	BAO	total
PL18 temp.+pol.	-1.1	-0.4	-7.0	-	-	-	-	-8.5
PL18	-1.0	-0.1	-3.1	+1.4	-	-	-	-2.8
PL18+ $f\sigma_8$	+0.1	-0.3	-5.6	+0.5	-8.3	-	-	-13.6
PL18+DESY1+BAO	-0.6	-0.8	-3.7	+0.3	-	-0.7	+0.8	-4.7
$f\sigma_8$ +DESY1+BAO	-	-	-	-	-1.2	-2.9	-2.2	-6.3
PL18+ $f\sigma_8$ +DESY1+BAO	-0.2	-1.1	-5.3	-0.7	-6.8	+0.8	+0.1	-13.2

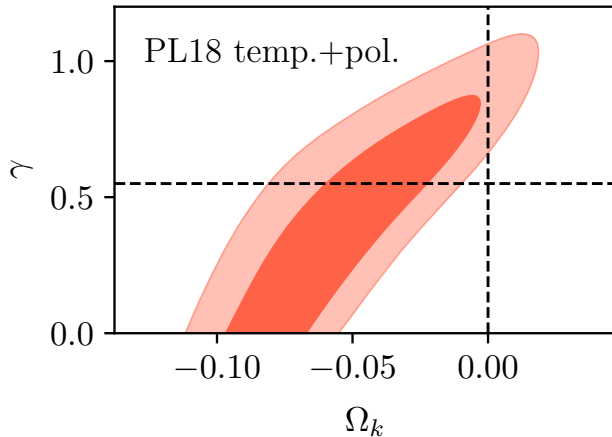


FIG. 4. Degeneracy between γ and Ω_K in the PL18 temp.+pol. analysis when both parameters are allowed to vary. Contours show the 68% and 95% credible intervals. The dashed lines mark the point $[\Omega_K = 0, \gamma = 0.55]$ corresponding to the concordance flat Λ CDM model.

data and that from the large-scale structure data can be reconciled with a high- γ model. Our findings indicate that these cosmological tensions can be interpreted as evidence of growth suppression.

A late-time growth suppression is not straightforward to achieve in modified theories of gravity, particularly if the expansion history is similar to that in the concordance model [67–69] as our constraints indicate. Nevertheless, there is sufficient freedom in the space of modified-gravity theory (within a sub-class of Horndeski models, e.g. [70–72]) to do so. Probing such modified-gravity theories should be within the reach of future surveys and experiments [73–75]. Specifically, upcoming large-scale structure data [76–81] will improve $f\sigma_8$ data both in terms of measurement precision and redshift coverage. In parallel, forthcoming CMB measurements [57, 82–84] with higher resolution and sensitivity will also play a significant role in pinning down the ex-

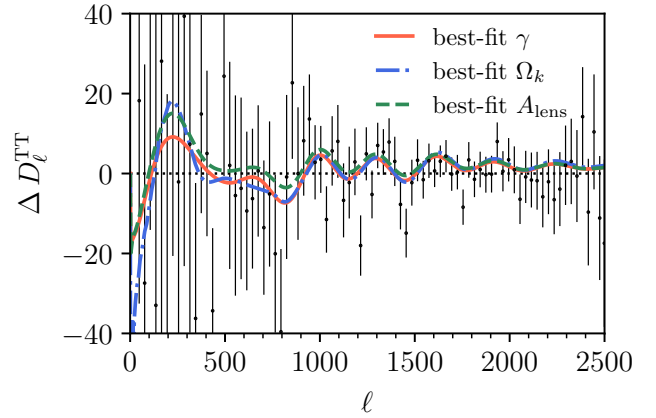


FIG. 5. Residuals in the CMB TT angular power spectrum $D_\ell \equiv \ell(\ell + 1)C_\ell/(2\pi)$ between the best-fit model with free γ (orange), best-fit model with curvature (blue), and best-fit model with free CMB lensing amplitude A_{lens} (green). The data points and error bars represent the Planck 2018 (binned) TT power spectrum residuals and the 68% uncertainties. All residuals are computed with respect to the best-fit concordance model.

pansion history and growth rate. As we enter the era of high-precision large-scale structure and CMB measurements, joint analyses of these data sets will hold the key to confirming any evidence for physics beyond the standard model.

We are grateful to Eiichiro Komatsu, Eric Linder, Jessie Muir, and Fabian Schmidt for valuable comments on the manuscript. MN thanks Alex Mead for helpful conversations on details and modifications of HMcode-2020. We thank Stéphane Ilić, Johannes Lange, and Antony Lewis for useful discussions. We acknowledge support from the Leinweber Center for Theoretical Physics, NASA grant under contract 19-ATP19-0058, DOE under contract DE-FG02-95ER40899, and the University of Michigan Research Computing Package. Our

analysis was performed on the Greatlakes HPC cluster, maintained by the Advanced Research Computing division, UofM Information and Technology Service. MN thanks John Thiels and Mark Champe for going above and beyond during their service. This work was initiated at the Aspen Center for Physics, which was supported by the National Science Foundation grant PHY-1607611. We thank the Aspen Center for their hospitality.

* nguyenmn@umich.edu

† huterer@umich.edu

- [1] E. Abdalla *et al.*, *JHEAp* **34**, 49 (2022), arXiv:2203.06142 [astro-ph.CO].
- [2] A. G. Riess, W. Yuan, L. M. Macri, D. Scolnic, D. Brout, S. Casertano, D. O. Jones, Y. Murakami, G. S. Anand, L. Breuval, T. G. Brink, A. V. Filippenko, S. Hoffmann, S. W. Jha, W. D'Arcy Kenworthy, J. Mackenty, B. E. Stahl, and W. Zheng, *ApJ* **934**, L7 (2022), arXiv:2112.04510 [astro-ph.CO].
- [3] N. Aghanim *et al.* (Planck), *Astron. Astrophys.* **641**, A6 (2020), [Erratum: *Astron. Astrophys.* 652, C4 (2021)], arXiv:1807.06209 [astro-ph.CO].
- [4] E. Di Valentino *et al.*, *Astropart. Phys.* **131**, 102604 (2021), arXiv:2008.11285 [astro-ph.CO].
- [5] D. Huterer, arXiv e-prints (2022), arXiv:2212.05003 [astro-ph.CO].
- [6] E. J. Ruiz and D. Huterer, *Phys. Rev. D* **91**, 063009 (2015), arXiv:1410.5832 [astro-ph.CO].
- [7] J. L. Bernal, L. Verde, and A. J. Cuesta, *J. Cosmology Astropart. Phys.* **2016**, 059 (2016), arXiv:1511.03049 [astro-ph.CO].
- [8] M. Moresco and F. Marulli, *Mon. Not. Roy. Astron. Soc.* **471**, L82 (2017), arXiv:1705.07903 [astro-ph.CO].
- [9] S. Basilakos and F. K. Anagnostopoulos, *European Physical Journal C* **80**, 212 (2020), arXiv:1903.10758 [astro-ph.CO].
- [10] K. Said, M. Colless, C. Magoulas, J. R. Lucey, and M. J. Hudson, *MNRAS* **497**, 1275 (2020), arXiv:2007.04993 [astro-ph.CO].
- [11] C. García-García, J. Ruiz-Zapatero, D. Alonso, E. Bellini, P. G. Ferreira, E.-M. Mueller, A. Nicola, and P. Ruiz-Lapuente, *J. Cosmology Astropart. Phys.* **2021**, 030 (2021), arXiv:2105.12108 [astro-ph.CO].
- [12] J. Ruiz-Zapatero, C. García-García, D. Alonso, P. G. Ferreira, and R. D. P. Grummitt, *MNRAS* **512**, 1967 (2022), arXiv:2201.07025 [astro-ph.CO].
- [13] M. White, R. Zhou, J. DeRose, S. Ferraro, S.-F. Chen, N. Kokron, S. Bailey, D. Brooks, J. García-Bellido, J. Guy, K. Honscheid, R. Kehoe, A. Kremin, M. Levi, N. Palanque-Delabrouille, C. Poppett, D. Schlegel, and G. Tarle, *J. Cosmology Astropart. Phys.* **2022**, 007 (2022), arXiv:2111.09898 [astro-ph.CO].
- [14] S.-F. Chen, M. White, J. DeRose, and N. Kokron, *J. Cosmology Astropart. Phys.* **2022**, 041 (2022), arXiv:2204.10392 [astro-ph.CO].
- [15] T. M. C. Abbott *et al.* (DES), arXiv e-prints, arXiv:2207.05766 (2022), arXiv:2207.05766 [astro-ph.CO].
- [16] S. Wang, L. Hui, M. May, and Z. Haiman, *Phys. Rev. D* **76**, 063503 (2007), arXiv:0705.0165 [astro-ph].
- [17] J. Dossett, M. Ishak, J. Moldenhauer, Y. Gong, A. Wang, and Y. Gong, *JCAP* **04**, 022 (2010), arXiv:1004.3086 [astro-ph.CO].
- [18] D. Rapetti, C. Blake, S. W. Allen, A. Mantz, D. Parkinson, and F. Beutler, *Mon. Not. Roy. Astron. Soc.* **432**, 973 (2013), arXiv:1205.4679 [astro-ph.CO].
- [19] A. Pouri, S. Basilakos, and M. Plionis, *JCAP* **08**, 042 (2014), arXiv:1402.0964 [astro-ph.CO].
- [20] J. Ruiz-Zapatero, B. Stölzner, B. Joachimi, M. Asgari, M. Bilicki, A. Dvornik, B. Giblin, C. Heymans, H. Hildebrandt, A. Kannawadi, *et al.*, *A&A* **655**, A11 (2021), arXiv:2105.09545 [astro-ph.CO].
- [21] J. Muir *et al.* (DES), *Phys. Rev. D* **103**, 023528 (2021), arXiv:2010.05924 [astro-ph.CO].
- [22] U. Andrade, D. Anbjagane, R. von Marttens, D. Huterer, and J. Alcaniz, *J. Cosmology Astropart. Phys.* **2021**, 014 (2021), arXiv:2107.07538 [astro-ph.CO].
- [23] P. J. E. Peebles, *The large-scale structure of the universe* (Princeton University Press, 1980).
- [24] F. Bernardeau, S. Colombi, E. Gaztañaga, and R. Scoccimarro, *Phys. Rep.* **367**, 1 (2002), arXiv:astro-ph/0112551 [astro-ph].
- [25] P. J. E. Peebles, *ApJ* **205**, 318 (1976).
- [26] A. P. Lightman and P. L. Schechter, *ApJS* **74**, 831 (1990).
- [27] A. Cooray, D. Huterer, and D. Baumann, *Phys. Rev. D* **69**, 027301 (2004), arXiv:astro-ph/0304268.
- [28] J. N. Fry, *Physics Letters B* **158**, 211 (1985).
- [29] L.-M. Wang and P. J. Steinhardt, *Astrophys. J.* **508**, 483 (1998), arXiv:astro-ph/9804015 [astro-ph].
- [30] E. V. Linder, *Phys. Rev. D* **72**, 043529 (2005), arXiv:astro-ph/0507263 [astro-ph].
- [31] E. V. Linder and R. N. Cahn, *Astropart. Phys.* **28**, 481 (2007), arXiv:astro-ph/0701317.
- [32] Y. Gong, *Phys. Rev. D* **78**, 123010 (2008), arXiv:0808.1316 [astro-ph].
- [33] A. Lewis, A. Challinor, and A. Lasenby, *ApJ* **538**, 473 (2000), arXiv:astro-ph/9911177 [astro-ph].
- [34] C. Howlett, A. Lewis, A. Hall, and A. Challinor, *J. Cosmology Astropart. Phys.* **1204**, 027 (2012), arXiv:1201.3654 [astro-ph.CO].
- [35] T. M. C. Abbott *et al.* (Dark Energy Survey), *Phys. Rev. D* **98**, 043526 (2018), arXiv:1708.01530 [astro-ph.CO].
- [36] Code available at this fork of CAMB: github.com/MinhMPA/CAMB_GammaPrime_Growth.
- [37] Strictly speaking, the integrated Sachs-Wolfe effect, a secondary CMB anisotropy sourced by gravitational redshift, is also sensitive to γ .
- [38] F. Beutler, C. Blake, M. Colless, D. H. Jones, L. Staveley-Smith, G. B. Poole, L. Campbell, Q. Parker, W. Saunders, and F. Watson, *MNRAS* **423**, 3430 (2012), arXiv:1204.4725 [astro-ph.CO].
- [39] D. Huterer, D. Shafer, D. Scolnic, and F. Schmidt, *JCAP* **1705**, 015 (2017), arXiv:1611.09862 [astro-ph.CO].
- [40] S. S. Boruah, M. J. Hudson, and G. Lavaux, *MNRAS* **498**, 2703 (2020), arXiv:1912.09383 [astro-ph.CO].
- [41] R. J. Turner, C. Blake, and R. Ruggeri, *MNRAS* **518**, 2436 (2023), arXiv:2207.03707 [astro-ph.CO].
- [42] C. Blake *et al.*, *Mon. Not. Roy. Astron. Soc.* **415**, 2876 (2011), arXiv:1104.2948 [astro-ph.CO].
- [43] C. Blake *et al.* (GAMA), *MNRAS* **436**, 3089 (2013), arXiv:1309.5556 [astro-ph.CO].
- [44] C. Howlett, A. J. Ross, L. Samushia, W. J. Percival, and

- M. Manera, MNRAS **449**, 848 (2015), arXiv:1409.3238 [astro-ph.CO].
- [45] T. Okumura *et al.*, PASJ **68**, 38 (2016), arXiv:1511.08083 [astro-ph.CO].
- [46] A. Pezzotta *et al.*, Astron. Astrophys. **604**, A33 (2017), arXiv:1612.05645 [astro-ph.CO].
- [47] S. Alam *et al.* (eBOSS), Phys. Rev. D **103**, 083533 (2021), arXiv:2007.08991 [astro-ph.CO].
- [48] Likelihood and data available at this fork of `cobaya`: github.com/MinhMPA/cobaya.
- [49] N. Aghanim *et al.* (Planck), A&A **641**, A5 (2020), arXiv:1907.12875 [astro-ph.CO].
- [50] F. Beutler, C. Blake, M. Colless, D. H. Jones, L. Staveley-Smith, L. Campbell, Q. Parker, W. Saunders, and F. Watson, MNRAS **416**, 3017 (2011), arXiv:1106.3366 [astro-ph.CO].
- [51] A. J. Ross, L. Samushia, C. Howlett, W. J. Percival, A. Burden, and M. Manera (BOSS), MNRAS **449**, 835 (2015), arXiv:1409.3242 [astro-ph.CO].
- [52] S. Alam *et al.* (BOSS), MNRAS **470**, 2617 (2017), arXiv:1607.03155 [astro-ph.CO].
- [53] `cobaya.readthedocs.io/en/latest/likelihood_bao.html`.
- [54] J. Torrado and A. Lewis, J. Cosmology Astropart. Phys. **2021**, 057 (2021), arXiv:2005.05290 [astro-ph.IM].
- [55] A. Lewis, arXiv e-prints (2019), arXiv:1910.13970 [astro-ph.IM].
- [56] H. Jeffreys, *Theory of Probability* (Oxford University Press, 1939).
- [57] S. Aiola *et al.* (ACT), J. Cosmology Astropart. Phys. **2020**, 047 (2020), arXiv:2007.07288 [astro-ph.CO].
- [58] C. Heymans *et al.* (Kilo-Degree Survey), A&A **646**, A140 (2021), arXiv:2007.15632 [astro-ph.CO].
- [59] A. Amon *et al.*, MNRAS **518**, 477 (2023), arXiv:2202.07440 [astro-ph.CO].
- [60] A. Leauthaud *et al.*, MNRAS **510**, 6150 (2022), arXiv:2111.13805 [astro-ph.CO].
- [61] M. J. Mortonson, W. Hu, and D. Huterer, Phys. Rev. D **79**, 023004 (2009), arXiv:0810.1744 [astro-ph].
- [62] Y. Gong, M. Ishak, and A. Wang, Phys. Rev. D **80**, 023002 (2009), arXiv:0903.0001 [astro-ph.CO].
- [63] E. Di Valentino, A. Melchiorri, and J. Silk, Nature Astronomy **4**, 196 (2020), arXiv:1911.02087 [astro-ph.CO].
- [64] E. Di Valentino, W. Giarè, A. Melchiorri, and J. Silk, Phys. Rev. D **106**, 103506 (2022), arXiv:2209.12872 [astro-ph.CO].
- [65] P. A. R. Ade *et al.* (Planck), Astron. Astrophys. **594**, A13 (2016), arXiv:1502.01589 [astro-ph.CO].
- [66] The preference for anomalous growth index in PL18 temp.+pol. data ($\Delta\chi^2 = -8.5$ in favor of the free- γ model over the concordance one) decreases once the CMB lensing reconstruction likelihood is included ($\Delta\chi^2 = -2.8$). A similar effect is observed for the case of varying A_{lens} .
- [67] A. Barreira, B. Li, C. M. Baugh, and S. Pascoli, Phys. Rev. D **86**, 124016 (2012).
- [68] A. Joyce, L. Lombriser, and F. Schmidt, Annual Review of Nuclear and Particle Science **66**, 95 (2016), arXiv:1601.06133 [astro-ph.CO].
- [69] J. A. Kable, G. Benevento, N. Frusciante, A. De Felice, and S. Tsujikawa, J. Cosmology Astropart. Phys. **2022**, 002 (2022), arXiv:2111.10432 [astro-ph.CO].
- [70] F. Piazza, H. Steigerwald, and C. Marinoni, J. Cosmology Astropart. Phys. **2014**, 043 (2014), arXiv:1312.6111 [astro-ph.CO].
- [71] L. Péreron, F. Piazza, C. Marinoni, and L. Hui, J. Cosmology Astropart. Phys. **2015**, 029 (2015), arXiv:1506.03047 [astro-ph.CO].
- [72] L. Perenon, J. Bel, R. Maartens, and A. de la Cruz-Dombriz, JCAP **06**, 020 (2019), arXiv:1901.11063 [astro-ph.CO].
- [73] N. Frusciante, S. Peirone, S. Casas, and N. A. Lima, Phys. Rev. D **99**, 063538 (2019), arXiv:1810.10521 [astro-ph.CO].
- [74] L. Perenon, S. Ilić, R. Maartens, and A. de la Cruz-Dombriz, A&A **642**, A116 (2020), arXiv:2005.00418 [astro-ph.CO].
- [75] Y. Wen, M. Nguyen, and D. Huterer, (in prep.).
- [76] E. da Cunha *et al.* (Taipan), PASA **34**, e047 (2017), arXiv:1706.01246 [astro-ph.GA].
- [77] K. Gebhardt *et al.* (HETDEX), ApJ **923**, 217 (2021), arXiv:2110.04298 [astro-ph.IM].
- [78] D. J. Schlegel *et al.* (DESI), arXiv e-prints , arXiv:2209.03585 (2022), arXiv:2209.03585 [astro-ph.CO].
- [79] M. Takada *et al.* (PFS), PASJ **66**, R1 (2014), arXiv:1206.0737 [astro-ph.CO].
- [80] R. Laureijs *et al.* (Euclid), arXiv e-prints , arXiv:1110.3193 (2011), arXiv:1110.3193 [astro-ph.CO].
- [81] D. J. Schlegel *et al.*, arXiv e-prints , arXiv:2209.04322 (2022), arXiv:2209.04322 [astro-ph.IM].
- [82] P. Ade *et al.* (Simons Observatory Collaboration), J. Cosmology Astropart. Phys. **2019**, 056 (2019), arXiv:1808.07445 [astro-ph.CO].
- [83] K. N. Abazajian *et al.* (CMB-S4), arXiv e-prints , arXiv:1610.02743 (2016), arXiv:1610.02743 [astro-ph.CO].
- [84] E. Ally, E. Allys *et al.* (LiteBIRD), arXiv e-prints , arXiv:2202.02773 (2022), arXiv:2202.02773 [astro-ph.IM].